Макрогетероциклы
http://macroheterocycles.isuct.ru

DOI: 10.6060/mhc190451f

Molecular Structure, Optical and Magnetic Properties of Iron Tetra(2,3–quinoxalino)porphyrazine $[(N\text{–MeIm})_2Fe^{I}\{T(2,3\text{–Q})Pz\}^{\bullet 3-}]\}^{\bullet 2-}$ Radical Dianions

Maxim A. Faraonov,[a@1] Nikita R. Romanenko,[a,b] Alexey V. Kuzmin,[c] Dmitri V. Konarev,[a@2] Salavat S. Khasanov,[c] and Rimma N. Lyubovskaya[a]

[a]*Institute of Problems of Chemical Physics RAS, 142432 Chernogolovka, Russia*
[b]*Moscow State University, 119991 Moscow, Russia*
[c]*Institute of Solid State Physics RAS, 142432 Chernogolovka, Russia*
[@1]*Corresponding author E-mail: maksimfaraonov@yandex.ru*
[@2]*Corresponding author E-mail: konarev3@yandex.ru*

*Iron(II) tetra(2,3-quinoxalino)porphyrazine, $Fe^{II}T(2,3\text{-Q})Pz$, was obtained using diaminomaleonitrile and o-phenylenediamine as starting materials. Reduction of $Fe^{II}T(2,3\text{-Q})Pz$ by sodium fluorenone ketyl in the presence of cryptand[2.2.2] and N-methylimidazole followed by precipitation of crystals leads to crystalline salt $\{cryptand[2.2.2](Na^+)\}_2\cdot[(N\text{-MeIm})_2Fe^{I}\{T(2,3\text{-Q})Pz\}^{\bullet 3-}]^{\bullet 2-}\cdot 3C_6H_4Cl_2\cdot 2H_2O$ (**1**). Molecular structure and properties of the $[(N\text{-MeIm})_2Fe^{I}\{T(2,3\text{-Q})Pz\}^{\bullet 3-}]^{\bullet 2-}$ radical dianions have been studied. Reduction of $Fe^{II}T(2,3\text{-Q})Pz$ is accompanied by strong blue shift of Soret band in spectrum of **1** but Q-band has close position to that in the spectrum of neutral macrocycle. There is an alternation of the C-N_{meso} bonds in the macrocycle in **1**, the difference between short and long C-N_{meso} bonds of 0.017 Å supports the formation of radical trianionic $T(2,3\text{-Q})Pz^{\bullet 3-}$ macrocycle. Coordination of N-methylimidazole molecules to iron (I) atoms with the Fe–N(imidazole) distance of 1.999(7) Å is observed. Both Fe^{I} atom and radical trianionic $\{T(2,3\text{-Q})Pz\}^{3\bullet -}$ macrocycle contribute to the EPR signal of **1**, which is well interpreted as the superposition of Lorentzian shaped lines with $g_1 = 2.0917$, $g_2 = 2.0679$, $g_3 = 2.0292$, $g_4 = 1.9991$ and $g_5 = 1.9922$. The lines with higher g-factor (g_1 and g_2) value can be attributed to low spin (S = 1/2) Fe^{I} whereas the lines with lower g-factor (g_4 and g_5) values can be attributed to the radical trianionic $\{T(2,3\text{-Q})Pz\}^{\bullet 3-}$ macrocycle. The line with intermediate g-factor value (g_3) can originate from the contribution of both components. The value of effective magnetic moment at 300 K (2.32 μ_B) indicates a contribution of two non-interacting S = 1/2 spins from iron(I) atoms and radical trianionic $\{T(2,3\text{-Q})Pz\}^{\bullet 3-}$ macrocycle. These spins weakly antiferromagnetically interact with Weiss temperature of –3 K.*

Keywords: Tetrapyrazinoporphyrazines, crystal structure, optical and magnetic properties, reduction, coordination.

Молекулярная структура, оптические и магнитные свойства дианион–радикальной соли тетра(2,3–хиноксалино)порфиразина железа $[(N\text{–MeIm})_2Fe^{I}\{T(2,3\text{–Q})Pz\}^{\bullet 3-}]^{\bullet 2-}$

М. А. Фараонов,[a@1] Н. Р. Романенко,[a,b] А. В. Кузьмин,[c] Д. В. Конарев,[a@2] С. С. Хасанов,[c] Р. Н. Любовская[a]

[a]*Институт проблем химической физики РАН, 142432 Черноголовка, Россия*
[b]*Московский государственный университет, 119991 Москва, Россия*
[c]*Институт физики твердого тела РАН, 142432 Черноголовка, Россия*
[@1]*E-mail: maksimfaraonov@yandex.ru*
[@2]*E-mail: konarev3@yandex.ru*

Тетра(2,3-хиноксалино)порфиразинат железа(II) ($Fe^{II}T(2,3\text{-Q})Pz$) получен при использовании диаминомалеонитрила и о-фенилендиамина в качестве прекурсоров. При восстановлении $Fe^{II}T(2,3\text{-Q})Pz$ натриевой солью кетила

*флуоренона в присутствии криптанда[2.2.2] и N-метилимидазола (N-MeIm) получена кристаллическая соль {криптанд[2.2.2](Na$^+$)}$_2$·[(N-MeIm)$_2$Fe^I{T(2,3-Q)Pz}$^{•3-}$]$^{•2-}$·3C$_6$H$_4$Cl$_2$·2H$_2$O (**1**). Исследованы молекулярная структура и свойства дианион-радикалов [(N-MeIm)$_2$Fe^I{T(2,3-Q)Pz}$^{•3-}$]$^{•2-}$. Восстановление Fe^{II}T(2,3-Q)Pz сопровождается сильным сдвигом полосы Соре в сторону больших энергий в спектре **1**, при этом сдвига Q-полосы не наблюдается. В макроцикле наблюдается чередование связей C-N$_{meso}$, разница между короткими и длинными связями C-N$_{meso}$ составляет 0.017 Å. Это подтверждает образование трианион-радикалов T(2,3-Q)Pz$^{•3-}$. Наблюдается координация молекул N-метилимидазола на атомы железа(I) с расстоянием Fe–N(имидазол) 1.999(7) Å. Вклад в сигнал ЭПР соли **1** вносят как атомы Fe^I, так и трианион-радикал {T(2,3-Q)Pz}$^{3•-}$ Этот сигнал представляет собой суперпозицию Лоренцевых линий с g_1 = 2.0679, g_2 = 2.0917, g_3 = 2.0292, g_4 = 1.9991 и g_5 = 1.9922. Линии с более высокими g-факторами (g_1 and g_2) обусловлены присутствием низкоспинового Fe^I (S = 1/2), а линии с g_4 и g_5 характерны для трианион-радикала. При этом линия с g_3 может быть обусловлена как вкладом от Fe^I, так и {T(2,3-Q)Pz}$^{•3-}$. Значение эффективного магнитного момента соли **1** при 300 K (2.32 μ_B) указывает на вклад двух невзаимодействующих спинов S = 1/2 от атомов Fe^I и трианион-радикалов {T(2,3-Q)Pz}$^{•3-}$. В соли **1** наблюдаются слабые антиферромагнитные взаимодействия спинов с температурой Вейса –3 K.*

Ключевые слова: Тетрапиразинопорфиразины, кристаллическая структура, оптические и магнитные свойства, восстановление, координация.

Introduction

Macroheterocycles (porphyrins, phthalocyanines, tetrapyrazinoporphyrazines and others) are a large family of organic compounds which can form complexes with metals.[1,2] Some of these macrocycles possess biological activity, and are used as dyes and materials for solar cells, optics and organic electronics.[3-6] Reduction or oxidation of these macrocycles lead to the appearance of unpaired electron density delocalized over macrocycle which can provide the realization of conducting properties or magnetic ordering of spins. Previously it was shown that oxidation of macrocycles lead to formation of compounds with quasi-one-dimensional metallic conductivity, if macrocycles have π–π stacking arrangement of the macrocycles.[7] Reduction chemistry of metal macrocycles have been studying only recently.[8-21]

Recently it was shown that in salts obtained by reduction of iron(II) phthalocyanine and iron(II) hexadecachlorophthalocyanine macrocycles pack in layers,[22,23] one-dimentional chains[22] or closely packed π-π stacking columns.[24] In these salts only iron(II) atomes are reduced, no electron transfer to the phthalocyanine macrocycles is observed even inspite of the presence of sixteen chlorine atoms on periphery of macrocycle which increase essentially acceptor propertie of the macrocycle.

Tetrapyrazinoporphyrazines (TPyzPzs) are analogues of phthalocyanine with eight additional nitrogen atoms in pyrazino-substituents, TPyzPzs macrocycle has stronger acceptor properties in comparison with Pc macrocycle.[6,25-28] Synthetic approaches to production TPyzPzs and their analogues were well developed[29] and several anionic compounds of tetrapyrazinoporphirazines were obtained till now.[30,31] The addition of benzo-groups to TPyzPzs by linear annulation leads to tetra(2,3-quinoxalino)porphyrazine, T(2,3-Q)Pz, which is even stronger acceptor then TPyzPzs.[32]

In this work we synthesized iron(II) tetra(2,3-quinoxalino)porphyrazine, Fe^{II}T(2,3-Q)Pz, and study the reduction of this porphyrazine in the presence of cryptand[2.2.2] and *N*-methylimidazole with following precipitation of crystals by *n*-hexane. Crystalline salt {cryptand[2.2.2](Na$^+$)}$_2$·[(*N*-MeIm)$_2$Fe^I{T(2,3-Q)Pz}$^{•3-}$]$^{•2-}$·3C$_6$H$_4$Cl$_2$·2H$_2$O (**1**) containing unusual [(*N*-MeIm)$_2$Fe^I{T(2,3-Q)Pz}$^{•3-}$]$^{•2-}$ radical dianions was obtained. That allows us to study for the first time the reduction effect on molecular structure, optical and magnetic properties of iron(II) tetra(2,3-quinoxalino) porphyrazine.

Experimental

Materials

Diaminomaleonitrile (Acros, 98 %), 2,3-dichloro-5,6-dicyano-1,4-benzoquinone (Sigma-Aldrich, 98 %), iron(II) acetate (Sigma-Aldrich, 98 %), 4,7,13,16,21,24-hexaoxa-1,10-diazabicyclo[8.8.8]hexacosane (cryptand[2.2.2], TCI chemicals, 98 %), trifluoroacetic acid (CF$_3$COOH, Acros, 99 %), *n*-butanol (Acros, 99 %), magnesium turnings (Acros, 99.9 %), *N*-methylimidazole (Acros, 99 %) and pyridine (Acros, 99 %) were used as received. Sodium fluorenone ketyl was obtained as described.[33] Solvents were purified in argon atmosphere. *o*-Dichlorobenzene (C$_6$H$_4$Cl$_2$) was distilled over CaH$_2$ under reduced pressure; hexane was distilled over Na/benzophenone, benzonitrile (C$_6$H$_5$CN) was distilled over Na/benzophenone under reduced pressure. The solvents were degassed and stored in a glove box. The crystals of **1** were stored in a glove box. KBr pellets for IR- and UV-Visible-NIR measurements were also prepared in the glove box. EPR and SQUID measurements were performed on polycrystalline samples of **1** sealed in 2 mm quarz tubes under 10^{-5} Torr.

Synthesis

Iron(II) tetra(2,3-quinoxalino)porphyrazine, Fe^{II}T(2,3-Q)Pz, was synthesized according to procedure in ref.[34] with some modifications.

Diiminosuccinonitrile (DISN) was synthesized by oxidation of diaminomaleonitrile (DAMN) as described in ref.[35] 2,3-Dicyanoquinoxaline was synthesized by condensation of DISN and *o*-phenylenediamine according to ref.[36]

2,3-Dicyanoquinoxaline (1 g, 5.6 mmol) was added to solution of *n*-butanol (50 mL) with dissolved magnesium (140 mg, 5.8 mmol) (dissolution was initiated by iodine crystal) and the stirred mixture was refluxed for 6 h. Solvent was evaporated under reduced pressure. After this the obtained Mg^{II} complex was demetallated by dissolution in CF$_3$COOH (15 mL). Acid was evaporated,

the residue was washed with water, methanol and dried. The obtained crude metal-free macroheterocycle, H_2T(2,3-Q)Pz, and iron(II) acetate (500 mg) were refluxed in pyridine for 3 h under argon. After cooling the reaction mixture was poured into water, filtered, and carefully washed with water, methanol and toluene. Powder was dried at 100 °C in a vacuum for 2 hours to remove pyridine and water to give Fe^{II}T(2,3-Q)Pz (60 % yield). Anal. found: C 62.57, N 29.30, H 2.04 %. Calcd. for $C_{40}H_{16}N_{16}Fe$: C 62.68, N 29.24, H 2.10. IR (KBr) ν cm^{-1}: 575w, 606m, 611m, 709s, 763s, 881w, 1050m, 1080w, 1111m, 1132s, 1141s, 1203m, 1229s, 1322w, 1357w, 1394w, 1446w, 1523m, 1561w, 1631w, 2608w, 2636w, 2920w, 2972m, 3063w. UV-Vis (KBr pellet) λ_{max} nm: 348, 478, 551, 714 nm.

Synthesis of crystalline salt ***1.*** Salt {cryptand[2.2.2](Na^+)}$_2$·[(*N*-MeIm)$_2$$Fe^I${T(2,3-Q)Pz}$^{\bullet 3-}$]$^{\bullet 2-}$·3$C_6H_4Cl_2$·2$H_2O$ (**1**) was obtained by reduction of 31.9 mg of Fe^{II}T(2,3-Q)Pz (0.042 mmol) by excess of sodium fluorenone ketyl (50 mg, 0.247 mmol) in the presence of two equivalents of cryptand[2.2.2] (31.6 mg, 0.084 mmol) and 0.5 ml of *N*-methylimidazole by stirring overnight at 100 °C till complete dissolution of parent macrocycle and the formation of deep-violet solution. The reaction solution of salt **1** was filtered in a 50 mL glass tube of 1.8 cm diameter with a ground glass plug, and 30 mL of hexane was layered over the solution. Slow mixing of two solvents during 1 month provided precipitation of crystals on the walls of the tube. The solvent was decanted from the crystals and they were washed with *n*-hexane. Metallic dark black blocks of **1** were obtained in 31 % yield.

The composition of **1** was determined from X-ray diffraction on single crystals. The analysis of the obtained crystals under microscope in a glove box as well as testing of several single crystals from each synthesis by X-ray diffraction showed that only one crystalline phase is formed. Elemental analysis cannot be used to determine the composition of the obtained crystals due to their high air sensitivity and an addition of oxygen during the procedure of elemental analysis.

General

UV-Visible-NIR spectra were measured in KBr pellets on a Perkin Elmer Lambda 1050 spectrometer in the 250-2500 nm range. FT-IR spectra were obtained in KBr pellets with a Perkin-Elmer Spectrum 400 spectrometer (400–7800 cm^{-1}). EPR spectra were recorded on polycrystalline samples of **1** from 4 up to 295 K with a JEOL JES-TE 200 X-band ESR spectrometer equipped with a JEOL ES-CT470 cryostat.

X-Ray Crystal Structure Determination

Crystal data of **1**: $C_{102}H_{116}C_{16}FeN_{24}Na_2O_{14}$, M_r = 2216.71 g·mol^{-1}, metallic dark black blocks, monoclinic, P $2_1/c$, a = 16.0049(14), b = 17.7053(8), c = 19.3596(16) Å, α = 90, β = 113.933(10), γ = 90°, V = 5014.3(7) $Å^3$, Z = 2, d_{calc} = 1.468 g·cm^{-3}, μ = 0.397 mm^{-1}, F(000) = 2316, max. $2\theta_{max}$ = 52.69°, reflections measured 26018, unique reflections 8368, R_{int} = 0.1214, reflections with $I > 2\sigma(I)$ = 8368, parameters refined 691, restraints 777, R_1 = 0.1430, wR_2 = 0.4072, G.O.F. = 1.087, CCDC 1911840.

The data were collected on an Oxford diffraction "Gemini-R" CCD diffractometer with graphite monochromated MoK_α radiation using an Oxford Instrument Cryojet system. Raw data reduction to F^2 was carried out using CrysAlisPro, Oxford Diffraction Ltd. The structures were solved by direct method and refined by the full-matrix least-squares method against F^2 using SHELX 2016[37] and Olex2.[38] Non-hydrogen atoms were refined in the anisotropic approximation. Positions of hydrogen were calculated geometrically.

Results and Discussion

Synthesis

2,3-Dicyanoquinoxaline is the most suitable precursor to obtain tetra(2,3-quinoxalino)porphyrazine macrocycle.[34] Iron(II) tetra(2,3-quinoxalino)porphyrazine, Fe^{II}T(2,3-Q)Pz, was synthesized by metalation of corresponding metal-free macrocycle which was obtained by demetallation of corresponding Mg^{II}T(2,3-Q)Pz complex. Mg^{II}T(2,3-Q)Pz was obtained by tetramerization of 2,3-quinoxaline in the presence of magnesium buthoxide in *n*-butanol. 2,3-Dicyanoquinoxaline was synthesized from diaminomaleonitrile (DAMN) by two stages as described in ref.[35,36] (Scheme 1).

Obtained iron(II) tetra(2,3-quinoxalino)porphyrazine was used in the synthesis without further purification due to extremely low solubility of this porphyrazine. It

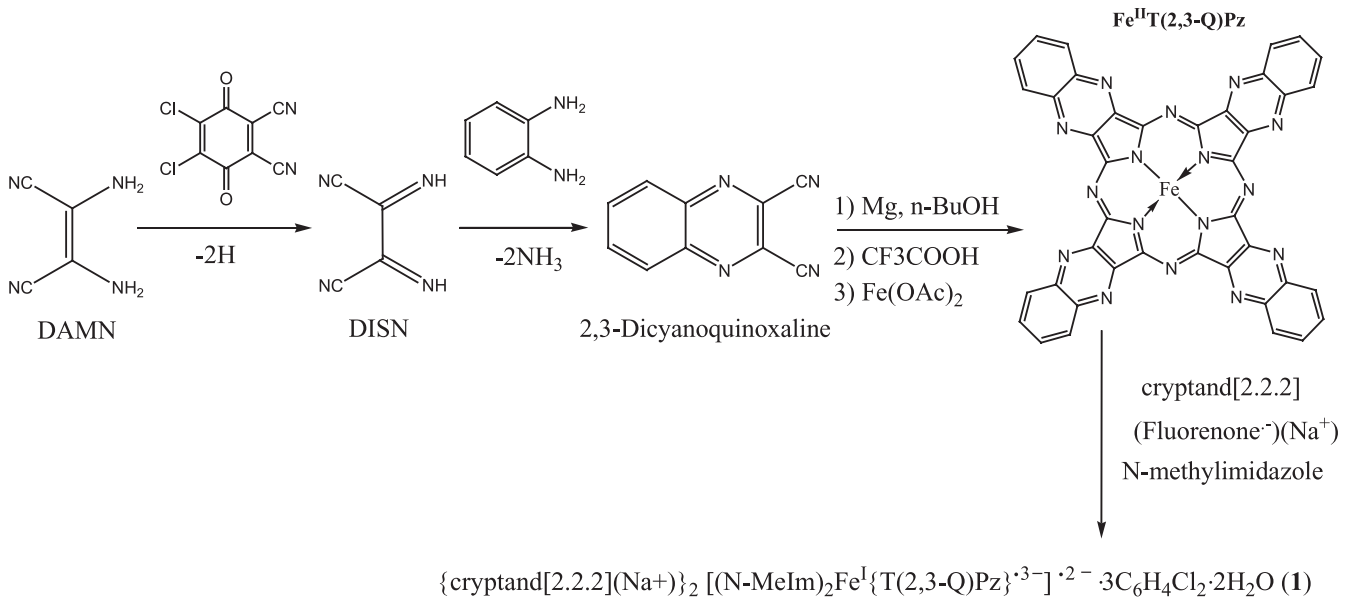

Scheme 1.

was reduced by an excess of sodium fluorenone ketyl in the presence of two equivalents of cryptand[2.2.2] and an excess of *N*-methylimidazole in *o*-dichlorobenzene. *N*-methylimidazole was added to increase the solubility of the salt in dichlorobenzene which is only partially soluble in this solvent without *N*-methylimidazole. In this case reduction results in complete dissolution of neutral $Fe^{II}T(2,3\text{-}Q)Pz$ and deep-violet solution is formed. Slow mixing of the obtained dichlorobenzene solution with *n*-hexane yields crystalline salt $\{cryptand[2.2.2](Na^+)\}_2 \cdot [(N\text{-}MeIm)_2Fe^I\{T(2,3\text{-}Q)Pz\}^{\bullet 3-}]^{\bullet 2-} \cdot 3C_6H_4Cl_2 \cdot 2H_2O$ (**1**) whose composition was determined from X-ray diffraction of single crystals. Several crystals tested from the synthesis have the same unit cell parameters indicating that only one crystal phase is formed. Water molecule forming hydrogen bond with the *N*-methylimidazole ligand can appear in the crystals of **1** most probably from pristine $Fe^{II}T(2,3\text{-}Q)Pz$ which was isolated using water and this water cannot be removed from the sample even under vacuum.

Earlier it was shown that reduction of titanyl tetra(acenaphthenopyrazino)porphyrazine ($Ti^{IV}OAceTPrzPz$) which has larger macrocycle by sodium fluorenone ketyl also leads to the formation dianionic species $\{O{=}Ti^{IV}(AceTPrzPz^{4-})\}^{2-}$.[31]

Spectra of Salts in the IR and UV-Visible-NIR Ranges

IR spectrum of **1** is a superposition of absorption bands of starting compounds (Figure S1, Table S1), some absorption bands are shifted slightly or change in intensity at the formation of the salt (Table S1).

Spectra of pristine $Fe^{II}T(2,3\text{-}Q)Pz$ and salt **1** in KBr pellets in the UV-Visible-NIR range are shown in Figure 1. Iron(II) phthalocianine ($Fe^{II}Pc$) shows one broad band in the visible range with the maximum at 662 nm.[22] $Fe^{II}T(2,3\text{-}Q)Pz$ shows larger number of bands in the UV-Visible-NIR range. The Soret band has maximum at 348 nm, the split *Q*-band is manifested at 478, 551 and 714 nm (Figure 1). The formation of **1** is accompanied by blue shift of Soret band to 318 nm, but *Q*-band in the spectrum of **1** has close position to that in the spectrum of neutral macrocycle and is observed as split band at 481, 563 and 717 nm. In spite of a close position contribution of the bands at 481 and 563 nm is essentially increases in comparison with the spectrum of pristine $Fe^{II}T(2,3\text{-}Q)Pz$ (Figure 1).

It was shown that reduction of unsubstituted tetrapyrazinoporphyrazine $H_2TPyzPz$ led to appearance of new intense absorption NIR band with maximum at 822 nm.[30] Characteristic for the reduced macrocycle absorption band in the NIR range is also observed in spectrum of $(PPN^+)_2\{O{=}Ti^{IV}(AceTPrzPz^{4-})\}^{2-}\cdot solv$ at 963 nm.[31] At the same time reduction of iron(II) phthalocyanine and iron(II) hexadecachlorophthalocyanine is metal-centered and is accompanied by the formation of iron(I) and iron(0) species without electron transfer to the phthalocyanine macrocycle.[22-24] As a result, the formation of $[Fe^IPc(-2)]^-$, $[Fe^ICl_{16}Pc(-2)]^-$ and $[FeCl_{16}Pc(-2)]_2^{3-}$ anions in solid state does not provide the appearance of new bands in the NIR range.[22-24] Absorption is also observed in the spectrum of **1** in the NIR range (shown by arc in Figure 1) but this absorption is not appeared as a separate band.

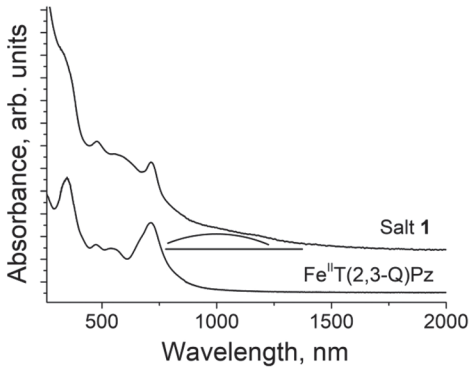

Figure 1. UV-Visible-NIR spectra of pristine $Fe^{II}T(2,3\text{-}Q)Pz$ and salt **1** in KBr pellets prepared for **1** in anaerobic conditions.

*Molecular Structure of $[(N\text{-}MeIm)_2Fe^I(T(2,3\text{-}Q)Pz)^{3\bullet-}]^{2\bullet-}$ and Crystal Structure of **1***

Salt **1** contains one independent half of radical dianions $[(N\text{-}MeIm)_2Fe^I\{T(2,3\text{-}Q)Pz\}^{\bullet 3-}]^{\bullet 2-}$, one independent cryptand[2.2.2](Na^+) cation, one and half *o*-dichlorobenzene molecule and one water molecule. The cryptand[2.2.2](Na^+) cation is disordered between two positions with 0.529(8) and 0.471(8) occupancies. Water molecule is positioned close to the hydrogen atom of the *N*-methylimidazole ligand and forms short hydrogen bond with it of 2.45 Å length.

Tetrapyrazinoporphyrazine macrocycle initially has stable aromatic 18 π-electron system. Its reduction is accompanied by the formation of less stable 19 π-electron system providing partial disruption of aromaticity of the macrocycle. That results in the alternation of the $C\text{-}N_{meso}$ bonds.[30,31] Studying of molecular structure of **1** shows that alternation of the $C\text{-}N_{meso}$ bonds is observed in the $[(N\text{-}MeIm)_2Fe^I\{T(2,3\text{-}Q)Pz\}^{\bullet 3-}]^{\bullet 2-}$ radical dianions (Figure 2a). Four shorter and four longer $C\text{-}N_{meso}$ bonds belong to two oppositely located isoindole units in **1**. The average difference between short and long bonds is 0.017 Å. Redistribution of the length of other bonds at the reduction is also observed. The average difference between short and long $C\text{-}N_{pyr}$ bonds is 0.012 Å. The average difference between short and long bonds $C\text{-}N_{meso}$ bonds in the $\{O{=}Ti^{IV}(AceTPrzPz^{4-})\}^{2-}$ and $H_2TPyzPz^{2-}$ dianions containing tetranionic and protonated dianionic macrocycles of 0.060 Å[31] and 0.092 Å[30] is essentially larger. Thus, disruption of aromaticity is less pronounced for the macrocycle in **1** compared with tetranionic and protonated dianionic TPrzPzs macrocycles. Nevertheless, the appearance of distortions of the macrocycle in **1** confirms formation of radical trianionic $T(2,3\text{-}Q)Pz^{\bullet 3-}$ macrocycles.

Macrocycle in **1** has saddle-like conformation, two benzopyrazine groups lie almost in 24-atom porphyrazine plane, but two other oppositely located groups come out above and below plane with displacement of atoms up to 0.398 Å. Iron(I) atoms lie exactly in 24-atom porphyrazine plane, the average distance $Fe\text{-}N_{pyr}$ is 1.962 Å. Coordination of *N*-methylimidazole molecules to iron(I) atoms is observed with the average N(imidazole)-Fe distance of 1.999(7) Å (Figure 2a).

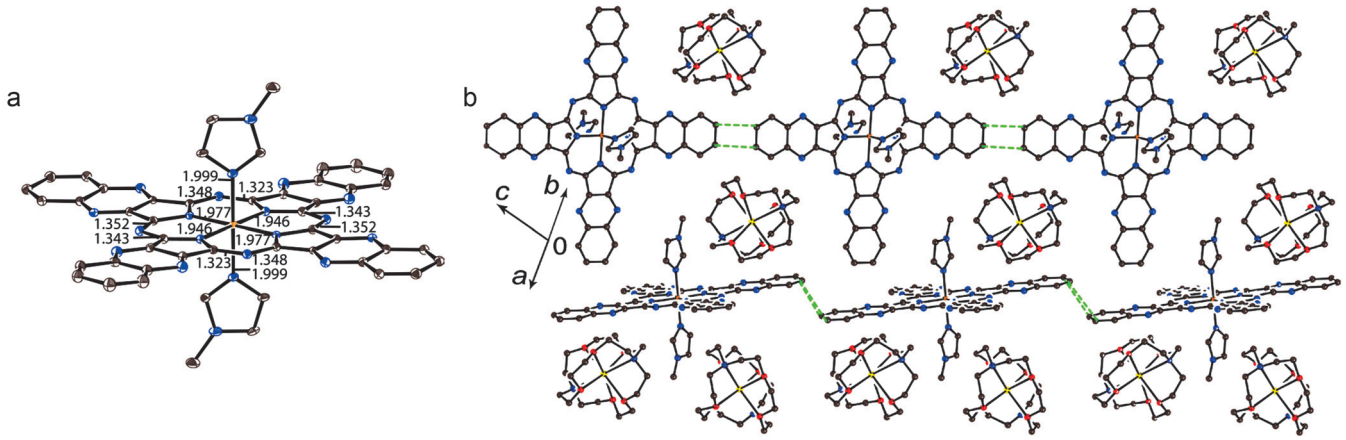

Figure 2. Molecular structure of radical dianions $[(N\text{-MeIm})_2Fe^{I}\{T(2,3\text{-Q})Pz\}^{\bullet 3-}]^{\bullet 2-}$ (a). Crystal structure of salt **1** (b). Van der Waals C···C contacts are shown by green dashed lines. Hydrogen atoms and solvent molecules are not shown for clarity.

In whole, salt **1** has a structure (Figure 2b) with one-dimensional chains formed by the $[(N\text{-MeIm})_2Fe^{I}\{T(2,3\text{-Q})Pz\}^{\bullet 3-}]^{\bullet 2-}$ radical dianions, each macrocycle has four side-by-side van der Waals (vdW) C···C contacts in these chains with neighboring ones of 3.435Å (are shown by green dashed lines in Figure 2b). These chains have perpendicular arrangement relative to each other as shown in Figure 2b. There is no short van der Waals contacts between the chains due to their isolation by bulky cryptand[2.2.2](Na^+) cations and solvent $C_6H_4Cl_2$ molecules (are not shown in Figure 2b).

Magnetic Properties

Magnetic properties of **1** were studied by EPR and SQUID techniques on a polycrystalline sample in anaerobic conditions.

Effective magnetic moment of salt **1** at 300 K is 2.32 μ_B that approximately corresponds to the contribution of two non-interacting $S = 1/2$ spin per formula unit (Figure 3a). These spins can originate from radical dianions $[(N\text{-MeIm})_2Fe^{I}\{T(2,3\text{-Q})Pz\}^{\bullet 3-}]^{\bullet 2-}$ containing iron(I) atoms with $S = 1/2$ spin state and radical trianionic $T(2,3\text{-Q})Pz^{\bullet 3-}$ macrocycle also with $S = 1/2$ spin state. Reciprocal magnetic susceptibility follows the Curie-Weiss law allowing the Weiss temperature to be estimated as –3 K (Figure 3b) indicating weak antiferromagnetic coupling of spins localized on Fe^{I} atom and delocalized over the macrocycle. Previously was even shown that such coupling between central paramagnetic metal atom and radical trianionic macrocycle can be rather weak.[13,14] Magnetic moment decreases slightly at cooling (Figure 3a) most probably due to weak antiferromagnetic coupling of spins.

Salt **1** manifests EPR signal which can be fitted well by five lines with Lorentzian line shape. Lines with $g_1 = 2.0679$ and $g_2 = 2.0917$ and the linewidth (ΔH) of 5.61 and 3.69 mT, respectively, were attributed to Fe^{I} with low ($S = 1/2$) spin state. Earlier it was shown that Fe^{I} with $S = 1/2$ spin state in generally manifests EPR signals with g-factor smaller than 2.3.[22-24] Narrower lines with $g_4 = 1.9991$ ($\Delta H = 1.17$ mT) and $g_5 = 1.9922$ ($\Delta H = 3.11$ mT) were attributed to the radical trianionic $T(2,3\text{-Q})Pz^{\bullet 3-}$ macrocycle, such asymmetric signals are generally characteristic for the reduced macrocycles.[13,14] There is also broad line with intermediate g-factor of 2.0292 ($\Delta H = 7.83$ mT). This g-factor is intermediate between those characteristic for Fe^{I} and radical trianionic macrocycles$^{3\bullet-}$ and, therefore,

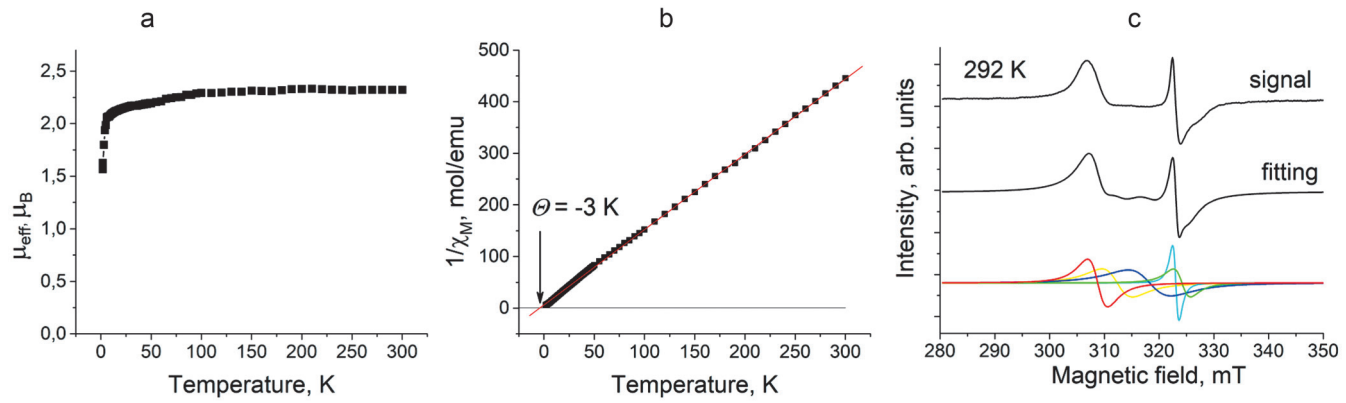

Figure 3. Temperature dependence of effective magnetic moment (a) and reciprocal molar magnetic susceptibility (b) for salt **1**. EPR spectrum of polycrystalline **1** at room temperature (c). This signal shape was preserved down to 4.2 K.

this component can be attributed to the contribution from both components. Thus, EPR spectra unambiguously show the presence of both paramagnetic species in **1**. The 5-line EPR spectrum of **1** is preserved down to 4.2 K. All components have nearly temperature independent *g*-factors and weakly temperature dependent linewidths as shown in Figure S2.

Conclusions

Thus, iron(II) tetra(2,3-quinoxalino)porphyrazine (Fe^{II}T(2,3-Q)Pz) was obtained using diaminomaleonitrile and *o*-phenylenediamine as starting materials. Reduction of Fe^{II}T(2,3-Q)Pz followed by precipitation of crystals leads to crystalline salt **1**. That allows us to study molecular structure and properties of the $[(N\text{-MeIm})_2Fe^{I}\{T(2,3\text{-Q})Pz\}^{\bullet 3-}]^{\bullet 2-}$ radical dianions. Reduction of Fe^{II}T(2,3-Q)Pz is accompanied by strong blue shift of Soret band and the appearance of weak NIR absorption in spectrum **1**. Disruption of aromaticity of macrocycle is observed which is manifested in the alternation of short and long the $C\text{-}N_{meso}$ bonds. Formation of **1** is accompanied by reduction of both iron(II) atoms and macrocycle to form the iron(I) atoms and radical trianionic $\{T(2,3\text{-Q})Pz\}^{\bullet 3-}$ macrocycles, the coordination of *N*-methylimidazole ligands to the iron(I) atoms is also observed. Formation of radical dianions $[(N\text{-MeIm})_2Fe^{I}\{T(2,3\text{-Q})Pz\}^{\bullet 3-}]^{\bullet 2-}$ with weakly interacting localized and delocalized spins is supported by SQIUD measurements. The formation of two different paramagnetic species is also supported by EPR spectra. It is known that iron(II) phthalocyanine has metal-centered first and second reduction and only third and forth reduction is centered on the macrocycle.[39] Obviously coordination of *N*-methylimidazole ligand changes such situation and double reduction is centered not only on the iron atoms but the macrocycle as well. Reduction of other iron(II) macrocycles in presence of different coordination ligands can yield anions with different value of charge transfer between iron atoms and the macrocycle and this work is now in progress.

Acknowledgements. The work was supported by Russian Science Foundation (project № 17-73-10199).

References

1. Kadish K.M., Smith K.M., Guilard R. *The Porphyrin Handbook, Vols. 1, 2, Chs. 10–13; Vol. 3, Ch. 25*. London: Academic Press, **2000**.
2. Milgrom L.R. *The Colors of Life: An Introduction to the Chemistry of Porphyrins and Related Compounds*. Oxford: Oxford University Press, **1997**. 249 p.
3. Mashiko T., Dolphin D. Porphyrins, Hydroporphyrins, Azaporphyrins, Phthalocyanines, Corroles, Corrins and Related Macrocycles. In: *Comprehensive Coordination Chemistry, Vol. 2* (Wilkinson G., Guilard R., McCleverty S.A., Eds.) Oxford: Pergamon Press, **1987**. p. 813–898.
4. Claessens C.G., Blau W.J., Cook M., Hanack M., Nolte R.J.M., Torres T., Wöhrle D. *Monatsh. Chem.* **2001**, *132*, 3–11.
5. Drain C.M., Varotto A., Radivojevic I. *Chem. Rev.* **2009**, *109*, 1630–1658.
6. Novakova V., Donzello M.P., Ercolani C., Zimcik P., Stuzhin P.A. *Coord. Chem. Rev.* **2018**, *361*, 1–73.
7. Inabe T., Tajima H. *Chem. Rev.* **2004**, *104*, 5503–5534.
8. Cissell J.A., Vaid T.P., Rheingold A.L. *Inorg. Chem.* **2006**, *45*, 2367–2369.
9. Wong E.W.Y., Leznoff D.B. *J. Porphyrins Phthalocyanines* **2012**, *16*, 154–162.
10. Wong E.W.Y., Walsby C.J., Storr T., Leznoff D.B. *Inorg. Chem*. **2010**, *49*, 3343–3350.
11. Zhou W., Platel R.H., Tasso T.T., Furuyama T., Kobayashi N., Leznoff D.B. *Dalton Trans.* **2015**, *44*, 13955–13961.
12. Konarev D.V., Khasanov S.S., Ishikawa M., Otsuka A., Yamochi H., Saito G., Lyubovskaya R.N. *Dalton Trans.* **2017**, *46*, 3492–3499.
13. Konarev D.V., Kuzmin A.V., Faraonov M.A., Ishikawa M., Nakano Y., Khasanov S.S., Otsuka A., Yamochi H., Saito G., Lyubovskaya R.N. *Chem. Eur. J.* **2015**, *21*, 1014–1028.
14. Konarev D.V., Faraonov M.A., Kuzmin A.V., Khasanov S.S., Nakano Y., Batov M.S., Norko S.I., Otsuka A., Yamochi H., Saito G., Lyubovskaya R.N. *New J. Chem.* **2017**, *41*, 6866–6874.
15. Konarev D.V., Troyanov S.I., Kuzmin A.V., Nakano Y., Ishikawa M., Faraonov M.A., Khasanov S.S., Litvinov A.L., Otsuka A., Yamochi H., Saito G., Lyubovskaya R.N. *Inorg. Chem.* **2017**, *56*, 1804−1813.
16. Konarev D.V., Kuzmin A.V., Khasanov S.S., Batov M.S., Otsuka A., Yamochi H., Kitagawa H., Lyubovskaya R.N. *CrystEngComm* **2018**, *20*, 385–401.
17. Konarev D.V., Kuzmin A.V., Khasanov S.S., Litvinov A.L., Otsuka A., Yamochi H., Kitagawa H., Lyubovskaya R.N. *Chem. Asian J.* **2018**, *13*, 1552–1560.
18. Konarev D.V., Khasanov S.S., Ishikawa M., Otsuka A., Yamochi H., Saito G., Lyubovskaya R.N. *Chem. Asian J.* **2017**, *12*, 910–919.
19. Konarev D.V., Khasanov S.S., Kuzmin A.V., Nakano Y., Ishikawa M., Otsuka A., Yamochi H., Saito G., Lyubovskaya R.N. *Cryst. Growth Des.* **2017**, *17*, 753–762.
20. Konarev D.V., Zorina L.V., Khasanov S.S., Litvinov A.L., Otsuka A., Yamochi H., Saito G., Lyubovskaya R.N. *Dalton Trans.* **2013**, *42*, 6810–6816.
21. Konarev D.V., Zorina L.V., Khasanov S.S., Hakimova E.U., Lyubovskaya R.N. *New J. Chem*. **2012**, *36*, 48–51.
22. Konarev D.V., Kuzmin A.V., Ishikawa M., Nakano Y., Faraonov M.A., Khasanov S.S., Otsuka A., Yamochi H., Saito G., Lyubovskaya R.N. *Eur. J. Inorg. Chem*. **2014**, *24*, 3863–3870.
23. Konarev D.V., Khasanov S.S., Ishikawa M., Otsuka A., Yamochi H., Saito G., Lyubovskaya R.N. *Inorg. Chem.* **2013**, *52*, 3851–3859.
24. Konarev D.V., Zorina L.V., Ishikawa M., Khasanov S.S., Otsuka A., Yamochi H., Saito G., Lyubovskaya R.N. *Cryst. Growth Des*. **2013**, *13*, 4930–4939.
25. Takahashi K., Aoki Y., Sugitani T., Moriyama F., Tomita Y., Handa M., Kasuga K., Sogabe K. *Inorg. Chim. Acta* **1992**, *201*, 247–249.
26. Ohta K., Watanabe T., Fujimoto T., Yamamoto I. *J. Chem. Soc., Chem. Commun.* **1989**, *21*, 1611–1613.
27. Lever A.B.P., Milaeva E.R., Speier G. The Redox Chemistry of Metallophthalocyanines in Solution. In: *Phthalocyanines: Properties and Applications, Vol. 3* (Leznoff C.C., Lever A.B. P., Eds.) New York: VCH Publishers, **1993**. p. 1–69.
28. Ruoff R.S., Kadish K.M., Boulas P., Chen E.C.M. *J. Phys. Chem*. **1995**, *99*, 8843–8850.
29. Donzello M.P., Ercolani C., Novakova V., Zimcik P., Stuzhin P.A. *Coord. Chem. Rev.* **2016**, *309*, 107–179.
30. Konarev D.V., Faraonov M.A., Kuzmin A.V., Fatalov A.M., Osipov N.G., Khasanov S.S., Shestakov A.F., Lyubovskaya R.N. *ChemistrySelect* **2018**, *3*, 4339–4343.

31. Faraonov M.A., Konarev D.V., Fatalov A.M., Khasanov S.S., Troyanov S.I., Lyubovskaya R.N. *Dalton Trans.* **2017**, *46*, 3547–3555.
32. Novakova V., Reimerova P., Svec J., Suchan D., Miletin M., Rhoda H.M., Nemykin V.N., Zimcik P. *Dalton Trans.* **2015**, *44*, 13220–13233.
33. Konarev D.V., Khasanov S.S., Yudanova E.I., Lyubovskaya R.N. *Eur. J. Inorg. Chem.* **2011**, *6*, 816–820.
34. Konarev D.V., Khasanov S.S., Ishikawa M., Yudanova E.I., Shevchun A.F., Mikhailov M.S., Stuzhin P.A., Otsuka A., Yamochi H., Saito G., Lyubovskaya R.N. *ChemistrySelect* **2016**, *1*, 323–330.
35. Webster O.W., Hartter D.R., Begland R.W., Shepparad W.A., Cairncross A. *J. Org. Chem*. **1972**, *37*, 4133–4136.
36. Begland R.W., Hartter D.R. *J. Org. Chem*. **1972**, *37*, 4136–4145.
37. Sheldrick G.M. *Acta Crystallogr., Sect. A: Found. Crystallogr.* **2008**, *64*, 112−122.
38. Dolomanov O.V., Bourhis L.J., Gildea R.J., Howard J.A.K., Puschmann H. *J. Appl. Crystallogr.* **2009**, *42*, 339−341.
39. Clack D.W., Yandle J.R. *Inorg. Chem.* **1972**, *11*, 1738–1742.

Received 30.04.2019
Accepted 15.05.2019